

## OPEN

# Preoperative Helical Dynamic Enhanced Multidetector Row Computed Tomography: Can It Be a Prognostic Indicator in Early-Stage Non-small Cell Lung Cancer?

Jung Won Moon, MD,\* Chin A Yi, MD,\* Kyung Soo Lee, MD,\* Sook Young Woo, MS,† O Jung Kwon, MD,‡ Ehwa Yang, PhD,\* Jae-Hun Kim, PhD,\* and Joungho Han, MD§

**Objective:** This study aimed to investigate the prognostic significance of dynamic contrast-enhanced computed tomography in patients with stage IA non-small cell lung cancer (NSCLC).

**Methods:** We retrospectively enrolled 139 patients (77 men, 62 women; mean age, 59 years) with stage IA NSCLC who underwent dynamic contrast-enhanced computed tomography. Data on age, pathologic subtype, peak enhancement, and net enhancement of primary lung cancer were collected and correlated with 5-year survival.

**Results:** Peak enhancement had a significant correlation with overall survival in the univariable analysis (hazard ratio [HR], 1.18, confidence interval [CI], 1.01–1.38;  $P = 0.04$ ) and in the multivariable analysis (HR, 1.19; CI, 1.01–1.39;  $P = 0.04$ ). Patients with peak enhancement of 90 Hounsfield unit or higher had a significantly increased risk of death compared with patients with less enhancement after curative surgery (HR, 4.15; CI, 1.23–13.95;  $P = 0.02$ ).

**Conclusions:** Our study confirmed the prognostic significance of peak enhancement as an indicator for the overall survival of stage IA NSCLC.

**Key Words:** NSCLC, DCE CT, peak enhancement, net enhancement, overall or progression-free or metastasis-free survival

(*J Comput Assist Tomogr* 2022;46: 308–314)

Tumor growth and metastasis require neoangiogenesis for its blood supply from preexisting vessels when a primary tumor grows beyond a few hundred micrometers to 1 mm in diameter.<sup>1,2</sup> Without angiogenesis, a tumor cannot expand its volume in the primary site and cannot metastasize to other sites. Therefore, tumors activate angiogenesis genes mainly through the vascular endothelial growth factor (VEGF) signaling the pathway to stimulate the formation of new blood vessels. Therefore, angiogenesis is an

essential step for tumor growth and has been a target of novel antiangiogenesis therapy in cancer treatment such as bevacizumab, anti-VEGF factor A antibody. Tumor angiogenesis can be directly measured by counting microvessel density (MVD) on pathologic slides of a surgical specimen. It is regarded as a quantitative biomarker of tumor growth and expected to play a role as a prognostic factor for the prediction of metastasis and survival. In breast, colon, and early-stage lung cancers, higher MVD correlates with a higher chance of metastasis and poorer prognosis.<sup>3–6</sup>

Helical dynamic computed tomography (CT) scan is considered to be one of the most useful diagnostic tools for the evaluation of malignant and benign nodules by demonstrating the higher peak enhancement (PE) and net enhancement (NE) in malignant nodules. The PE of malignant nodules showed a significant correlation with VEGF and MVD.<sup>7,8</sup> Microvessel density in malignant nodules is considered to play a role as a prognostic indicator in non-small cell lung cancer (NSCLC). Several studies show that tumor neoangiogenesis, as measured by MVD, is a prognostic factor for both overall and disease-free survival in lung cancer. The extent of tumor enhancement on CT, which can be measured non-invasively and repeatedly, is correlated with VEGF expression in NSCLC.<sup>9</sup> However, there has been no report that can demonstrate the direct correlation between the extent of enhancement on CT and the prognosis of early NSCLC.

We aimed to evaluate the value of dynamic enhancement as a prognostic factor in stage IA NSCLC, through analyzing the relationship of the extent of enhancement of NSCLC with overall (OS), progression-free (PFS), and metastasis-free survival (MFS) after curative surgery.

## MATERIALS AND METHODS

### Patients

An institutional review board approved this study with a waiver of informed consent. From 2003 to 2007, 706 patients with suspected solitary pulmonary nodule underwent helical dynamic CT. Excluding typical benign nodules based on CT images such as nodules with benign features of calcification or fat internal characteristics ( $n = 59$ ), patients with nodules that have a possibility of malignancy ( $n = 647$ ) were candidates for percutaneous needle biopsy. Percutaneous needle biopsy was feasible in 376 patients. If percutaneous needle biopsy was not feasible, regular observation or biopsy for any extrathoracic lesions with a possibility of malignancy was done (Fig. 1).

Among patients who could have pathologic diagnosis for a solitary pulmonary nodule, 218 nodules were confirmed as NSCLC. Other nodules included benign nodules ( $n = 118$ ), metastasis from extrathoracic malignancy ( $n = 35$ ), and small cell lung cancer ( $n = 5$ ). After conventional workup such as physical examination, laboratory tests, bronchoscopy, mediastinoscopic biopsy, and positron emission tomography/CT, curative surgery was performed in

From the \*Department of Radiology, †Biostatistics Unit, Samsung Biomedical Research Institute, ‡Division of Respiratory and Critical Care Medicine, Department of Internal Medicine, and §Department of Pathology, Samsung Medical Center, Sungkyunkwan University School of Medicine, Seoul, Korea. Received for publication February 8, 2021; accepted June 24, 2021.

Correspondence to: Chin A Yi, MD, Department of Radiology, Samsung Medical Center, Sungkyunkwan University School of Medicine, Seoul 06351, Korea (e-mail: cayi@skku.edu).

Present address: Jung Won Moon, MD, Department of Radiology, Kangnam Sacred Heart Hospital, Hallym University School of Medicine, Seoul 07441, Korea.

This work was supported by a National Research Foundation of Korea grant funded by the Korean government (MEST; NRF-2019R1A2C1011183); this funding source had no involvement in the conduct of the research and the preparation of the article. Otherwise, the authors declare no conflict of interest.

Copyright © 2022 The Author(s). Published by Wolters Kluwer Health, Inc. This is an open-access article distributed under the terms of the Creative Commons Attribution-Non Commercial-No Derivatives License 4.0 (CCBY-NC-ND), where it is permissible to download and share the work provided it is properly cited. The work cannot be changed in any way or used commercially without permission from the journal.

DOI: 10.1097/RCT.0000000000001270

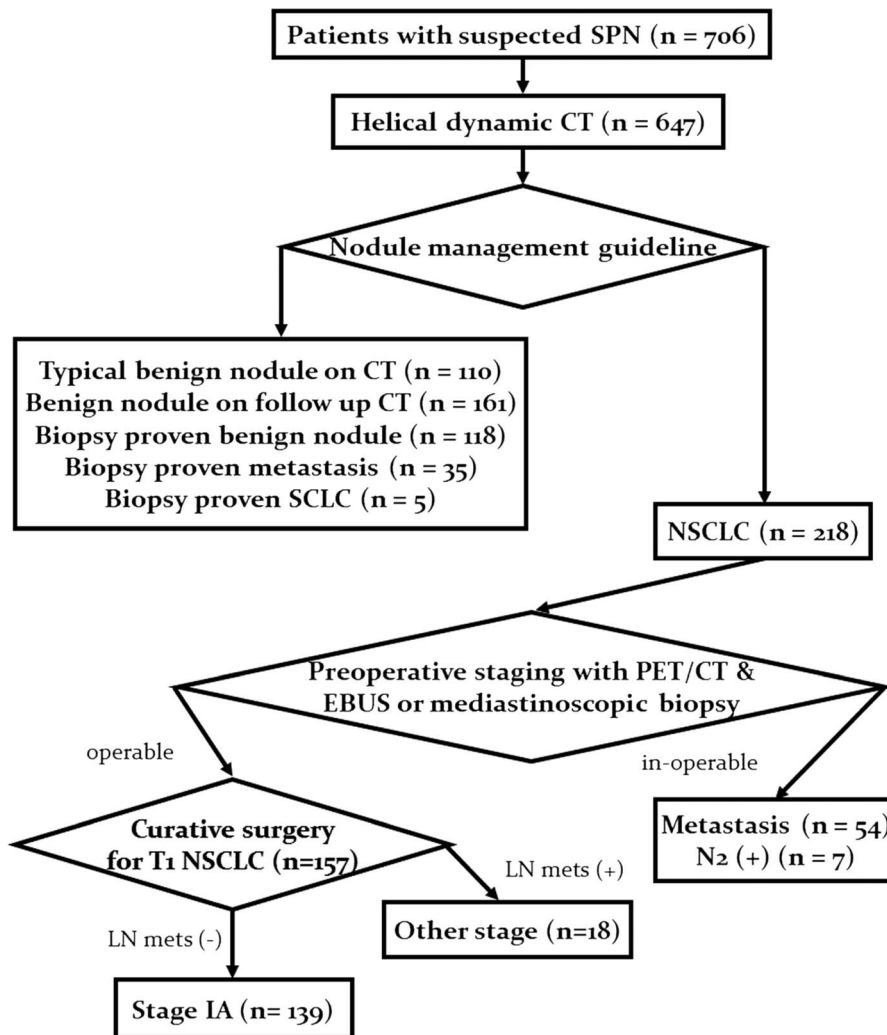


FIGURE 1. Flow sheet showing patient selection.

157 patients. Inoperable patients include the presence of N2 nodes (n = 7) or distant metastasis (n = 54). Finally, 139 patients (male-to-female ratio, 77:62; mean age, 59 years; range, 24–81 years) who underwent preoperative dynamic contrast-enhanced CT and subsequent curative surgery were included in this study. About 25% of this study population has been previously reported in the article by Jeong et al.<sup>10</sup> In this study, Jeong et al analyzed the diagnostic efficacy of helical dynamic CT for the differentiation of benign and malignant nodules, but this study did not analyze the survival of this study population.

### Image Acquisition and Analysis

Targeted thin-section CT scans were performed around nodules with the helical technique (120 kVp; 90 mA; 0.8-seconds gantry rotation time; beam width, 10 mm; table speed, 13.75 mm per rotation; reconstruction performed with a bone algorithm; and 1.25-mm section thickness) before intravenous contrast administration. Dynamic images on a 30-second interval (30, 60, 90, and 120 seconds) and delayed images on 5 and 15 minutes were obtained after contrast administration (with an infusion rate of 3 mL/s, for a total of 120 mL of Iomeron 300 [Iomeprol]; Bracco, Milan, Italy) with a power injector (MCT Plus; Medrad, Pittsburgh, Pennsylvania).

For clinical staging, helical CT scans (120 kVp; 125 mA; beam width, 20 mm; table speed, 27.5 mm per rotation; reconstruction with a bone algorithm; and 5 mm thick) were performed after a dynamic study, covering the whole lung and upper abdomen at the level of the middle pole of both kidneys.

All CT scans were directly displayed with 2.5-mm reconstructed slice thickness on the picture archiving and communication system (MT; General Electric Medical Systems Integrated Imaging Solutions, Prospect, Illinois).

Two thoracic radiologists (with 5 and 17 years of experience in chest CT scan interpretation) reviewed chest CTs. We picked a 2-dimensional axial image with the largest long axis of the nodule on the picture archiving and communication system, and then measured the size on lung window setting and the attenuation value (in Hounsfield unit [HU]) on mediastinal window setting with 2.5-mm slice thickness for the analysis of the nodule. The heterogeneity of nodule attenuation can be resulted from necrosis, cystic degeneration, calcification, and ground-glass attenuation, and even partial volume of the nodule on some slices can cause attenuation measurement error especially for small nodules. Thus, to get adequate attenuation revealing the most proliferative MVD foci, we put the maximum-sized region of interest over the highest attenuation portion of nodule at each given acquisition time point,

from unenhanced images to 15-minute images. Parameters from dynamic enhancement characteristics were values of PE and NE (PE – unenhanced attenuation). The phase of brightest attenuation was chosen for the PE measurement.

### Prognosis Evaluation

Overall survival, PFS, and MFS were evaluated on an electronic chart review. Overall survival was defined as an interval between the CT acquisition date and the date of death or last follow-up date. Disease progression was defined as 1 of 3 occasions: (a) the intrathoracic recurrent mass around the stump area, lymphadenopathy, or pleural seeding; (b) new metastasis on dedicated imaging or pathology; or (c) death. Progression-free survival was defined as an interval between the CT acquisition date and the first presentation of progression. Metastasis-free survival was defined as an interval between the CT acquisition date and new metastasis. Median follow-up period was 74 months.

### Statistical Analysis

Possible prognostic indicators for OS, PFS, and MFS were evaluated in terms of age, sex, pathology, and the parameters from dynamic helical CT (PE and NE). The pathologic type was divided into adenocarcinoma and others. The unit changes of PE and NE values were regarded as the 10-HU increase or decrease in CT attenuation.

Univariable and multivariable analyses were done. Overall survival was estimated using Cox regression analysis. Efron method was used to handle ties in the failure time. The proportional hazards assumption was confirmed by examining the log (–log[survival]) curves and by testing the partial (Schoenfeld) residuals, and no relevant violations were found.<sup>11</sup> Competing regression analysis was used for PFS and MFS. Death was regarded as a competing risk. The proportional hazards assumption was confirmed by examining the log (–log[1 – CIF]) plot against log(time), where CIF is the cumulative incidence function for the progression. Because PE had multicollinearity with NE, multivariable analysis was performed separately for each (one time with only PE included and the other time with only NE included).

Cutoff values were decided using the log-rank test to indicate the level of the largest drop of survival.<sup>12</sup> Patients with enhancing nodules more than the cutoff values of PE or NE were considered as a high-risk group. Likewise, patients with less enhancing nodules were considered as a low-risk group for OS, PFS, and MFS.

In all tests, a *P* value <0.05 was statistically significant. Statistical analysis was performed using SAS 9.3 (SAS Institute Inc, Cary, North Carolina) and 'cmprsk' package in R 3.0.1 (R Foundation for Statistical Computing, Vienna, Austria; <http://www.R-project.org/>).

## RESULTS

### Patient Characteristics

Patients' characteristics are demonstrated in Table 1 (*n* = 139). Adenocarcinoma accounts for the majority of pathologic-type lung cancer (*n* = 114), followed by squamous cell carcinoma (*n* = 17), large cell neuroendocrine carcinoma (*n* = 4), pleomorphic carcinoma (*n* = 2), and adenosquamous carcinoma (*n* = 2). Mean size of the 139 nodules was 21 ± 5.7 mm (range, 6–30 mm).

Twenty-six patients died on follow-up. Eight patients showed local recurrence at stump. One patient had both local recurrence and metastasis. Thirty-six patients showed new metastasis in 63 sites. Lung-to-lung metastasis was most common (*n* = 33; median duration, 76 months), followed by bone (*n* = 9; median duration, 20 months), brain (*n* = 8; median duration, 20 months), lymph node (*n* = 4; median duration, 39 months), cerebrospinal fluid

**TABLE 1.** Patient Characteristics: Clinical Features and CT Findings (*n* = 139)

Characteristics	n
Age (mean, range), y	59 (24–81)
Sex, %	
Male	77 (55.4)
Female	62 (44.6)
Pathology, %	
Adenocarcinoma	114 (82.0)
Squamous cell carcinoma	17 (12.2)
Large cell neuroendocrine carcinoma	4 (2.9)
Pleomorphic carcinoma	2 (1.4)
Adenosquamous carcinoma	2 (1.4)
Prognosis, %	
Progression-free	86 (61.9)
Progression	53 (38.1)
Death	26 (18.7)
Local recurrence	8 (5.8)
Metastasis	36 (28.8)
CT findings, mean ± SD (range)	
Size, mm	21 ± 5.7 (6–30)
NE, HU	53 ± 18.5 (11–147)
PE, HU	97 ± 21 (42–189)

(*n* = 3; median duration, 24 months), adrenal gland (*n* = 1; median duration, 31 months), peritoneum (*n* = 1; median duration, 31 months), kidney (*n* = 1; median duration, 25 months), back muscle (*n* = 1; 23 median duration, months), ureter (*n* = 1; 10 median duration, months), and liver (*n* = 1; median duration, 6 months).

Median survival was as follows: OS, 77 months (range, 1–102 months); PFS, 74 months (range, 1–102 months); and MFS, 75 months (range, 1–102 months).

### Univariable and Multivariable Analyses Regarding Survival

On univariable analysis, age and PE were significantly associated with OS (Table 2). Older patients showed worse OS (hazard ratio [HR], 1.05; confidence interval [CI], 1.01–1.09; *P* = 0.01). Larger PE value was a worse prognostic factor for OS (HR, 1.18; CI, 1.01–1.38; *P* = 0.04). Adenocarcinoma showed a high HR of 2.26 but was not significant. Net enhancement was not a significant factor for OS. Neither NE nor PE was a significant factor for PFS and MFS.

Multivariable analyses are demonstrated in Table 3, including PE and NE in turn. Peak enhancement was significantly correlated with OS (HR, 1.19; CI, 1.01–1.39; *P* = 0.04), but not for PFS and MFS (*P* > 0.05). Age was a significant prognostic factor on multivariable analysis including NE (HR, 1.04; CI, 1.00–1.08; *P* = 0.04). Sex, pathology, and NE were not significant factors in multivariable analysis regarding OS, PFS, and MFS.

### Cutoff Value Differentiating High- and Low-Risk Groups

For OS, the cutoff value was determined at 90 HU of PE, which showed the significant drop of survival (*P* = 0.01, Fig. 2). Thus, PE of 90 HU could be the cutoff value differentiating high- and low-risk groups (Fig. 3). Stage IA NSCLC with high PE

**TABLE 2.** Univariable Analysis Regarding OS and PFS

Variables	OS*		PFS†		MFS‡	
	HR (95% CI)	P	HR (95% CI)	P	HR (95% CI)	P
Age‡	<b>1.05 (1.01–1.09)</b>	<b>0.01</b>	0.98 (0.95–1)	0.07	0.98 (0.95–1.01)	0.28
Sex§	0.44 (0.19–1.05)	0.06	0.95 (0.52–1.71)	0.85	1.03 (0.53–1.98)	0.93
Pathology	2.26 (0.98–5.20)	0.06	0.55 (0.22–1.4)	0.21	0.74 (0.29–1.93)	0.54
Peak¶	<b>1.18 (1.01–1.38)</b>	<b>0.04</b>	1.02 (0.88–1.17)	0.82	1.05 (0.91–1.21)	0.51
Net¶	1.14 (0.96–1.36)	0.13	1.12 (0.97–1.28)	0.12	1.12 (0.97–1.29)	0.14

Bold items are statistically significant results.  
 \*Cox regression model was used.  
 †Competing regression model was used.  
 ‡Older age.  
 §Female sex.  
 ||Adenocarcinoma versus others.  
 ¶Per 10 HU.

(>90 HU) showed more than 4 times increased risk of death in OS than stage IA NSCLC with less than 90 HU PE (Table 4; HR, 4.15; CI, 1.23–13.95; P = 0.02; Fig. 4).

**DISCUSSION**

Tumor angiogenesis is a major mechanism of tumor growth, recurrence, and metastasis, thus the antiangiogenic cancer therapy using direct and indirect angiogenesis inhibitors improved survival in the treatment of NSCLC.<sup>13–15</sup> In patients with lung cancer, the extent of tumor angiogenesis measured using the microvessel count and VEGF expression are generally accepted as an indicator of tumor aggressiveness and survival,<sup>3,4,9</sup> but these parameters can only be quantified based on the surgical specimen. Computed tomography

scans play an efficient and significant role in the diagnosis and follow-up surveillance of lung cancer.<sup>16,17</sup> The extent of tumor enhancement on CT scans can be measured repeatedly and noninvasively and quantified as a parameter of tumor vascularity.<sup>7,18,19</sup>

In this study, we demonstrate the PE on helical dynamic CT as a significant predictor of OS in stage IA NSCLC. Patients with a PE value more than 90 HU are presumed to have 4 times higher risk of death after curative surgery than patients with a PE value lower than 90 HU (HR, 4.15; CI, 1.23–13.95). Although we did not measure the MVD or VEGF on surgical specimens of our patients for the correlation with PE or NE, consistent results were expected with the prior study showing a significant correlation between PE and MVD or VEGF.<sup>7</sup> Tateishi et al<sup>19</sup> also suggested the significant correlation between PE and VEGF expression,

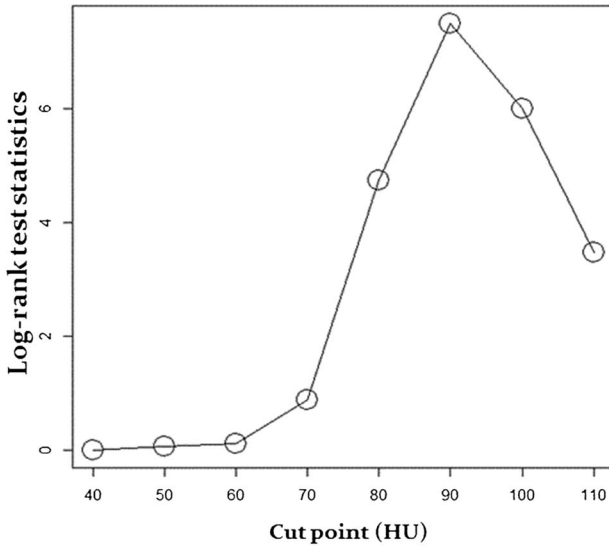
**TABLE 3.** Multivariable Analysis Regarding OS and PFS

Variables	OS*		PFS†		MFS‡	
	HR (95% CI)	P	HR (95% CI)	P	HR (95% CI)	P
Age‡	1.04 (0.99–1.08)	0.06	0.97 (0.95–1)	0.08	0.98 (0.95–1.02)	0.28
Sex§	0.55 (0.22–1.37)	0.2	0.76 (0.41–1.42)	0.39	0.91 (0.47–1.78)	0.79
Pathology	1.74 (0.71–4.25)	0.23	0.59 (0.23–1.53)	0.28	0.81 (0.3–2.17)	0.68
Peak¶	<b>1.19 (1.00–1.03)</b>	<b>0.04</b>	1.04 (0.91–1.18)	0.6	1.06 (0.93–1.22)	0.37

Variables	OS*		PFS†		MFS‡	
	HR (95% CI)	P	HR (95% CI)	Variables	HR (95% CI)	P
Age‡	<b>1.04 (1.00–1.08)</b>	<b>0.04</b>	0.97 (0.94–1)		0.98 (0.95–1.02)	0.28
Sex§	0.56 (0.23–1.4)	0.22	0.75 (0.41–1.39)		0.9 (0.46–1.77)	0.76
Pathology	1.8 (0.73–4.4)	0.2	0.62 (0.24–1.59)		0.84 (0.32–2.24)	0.73
Net¶	1.16 (0.99–1.03)	0.08	1.12 (0.98–1.29)		1.12 (0.97–1.3)	0.12

Bold items are statistically significant results.  
 Because PE had multicollinearity with NE, multivariable analysis was performed separately for each (one time with only PE included and the other time with only NE included).  
 \*Cox regression model was used.  
 †Competing regression model was used.  
 ‡Older age.  
 §Female sex, compared with male.  
 ||Adenocarcinoma versus others.  
 ¶Per 10 HU.



**FIGURE 2.** Log-rank test to compare the survival distribution at different cutoff points of PE. The most significant expression cutoff for survival analysis was the PE at 90 HU.

and the significant correlation between PE in VEGF-positive tumor and MVD. Therefore, this study extends upon the correlation between PE and MVD to investigate the clinical relevance of PE as a prognostic indicator for lung cancer survival.

Peak enhancement showed a significant correlation with prognosis; lung cancer patients with PE higher than 90 HU showed a higher risk of death on follow-up after curative surgery for stage IA NSCLC, but NE did not. Net enhancement is the difference between PE and the attenuation value on precontrast images. Peak enhancement is the highest enhancement value on multiphase dynamic enhancement CT. We presume that precontrast attenuation values also can reveal denser tumor vasculature or denser tumor cellularity in more aggressive lung cancers by showing higher precontrast attenuation values and subsequently minimizing the effect of NE in tumor angiogenesis when subtracting the precontrast attenuation values. When NE was correlated with the direct markers for tumor angiogenesis, it showed a weak correlation with MVD or VEGF in the previous study.<sup>7</sup>

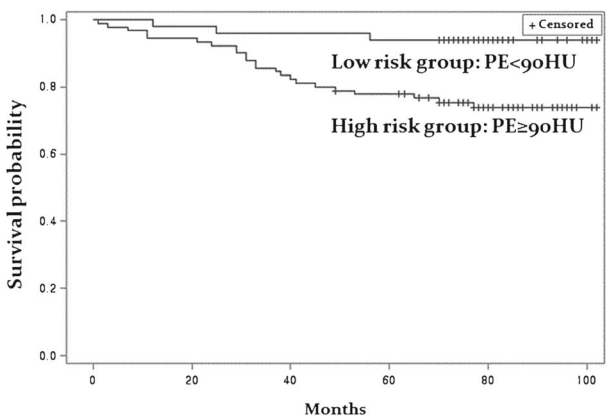


**FIGURE 3.** Overall survival curves separated by the cutoff value 90 HU PE. Patients with stage IA lung cancers that were enhanced more than 90 HU at its PE on CT showed poorer survival than patients who had stage IA lung cancer with less enhancement.

**TABLE 4.** Multivariable Analysis Regarding Peak Value 90 HU as the Cutoff

Variables	OS*	
	HR (95% CI)	P
Age†	0.53 (0.21–1.34)	0.18
Sex‡	1.04 (1–1.08)	0.08
Pathology§	1.41 (0.57–3.49)	0.46
Peak	<b>4.15 (1.23–13.95)</b>	<b>0.02</b>

Bold items are statistically significant results.

\*Cox regression analysis was done.

†Older age.

‡Female sex, compared with male.

§Adenocarcinoma versus others.

||Less than 90 HU versus more than 90 HU.

We included only stage IA NSCLC because the effect of tumor angiogenesis on patients' survival can be clearly seen when the stages of lung cancer are all the same within the study group of patients, because the stages are the well-known splitters for patients' survival. Other factors that may have effect on survival such as age, sex, and pathologic subtype were also included in the multivariate analysis, and PE was found as an independent factor for the prediction of patients' survival.

For PFS and MFS, however, PE did not show a significant correlation in this study. Fontanini et al<sup>3</sup> suggested that the microvessel count was correlated with hilar and mediastinal node metastasis on initial diagnosis and distant metastasis on 2-year follow-up. Tateishi et al<sup>19</sup> also demonstrated that PE of a tumor was significantly greater in N1–2 stage than N0. These prior studies included advanced cases that had grown with neoangiogenesis, which facilitate the invasion of the extracellular matrix and the subsequent vascular dissemination of tumor cells. In contrast, we included only early lung cancers, which were surgically removed at the time of diagnosis; thus, the number of tumors with vascular invasion was presumed relatively small in number and extent, compared with advanced lung cancers, so the chance of metastasis on follow-up was also decreased. If we follow up a longer period of time like a 10-year survival rate, higher PE might be found as a significant risk factor for the longer PFS or MFS.

Adenocarcinoma showed a broad range of HR from 0.98 to 5.2 for OS, compared with other NSCLC types. The International Association for the Study of Lung Cancer, the American Thoracic Society, and the European Respiratory Society classified a broad range of histologic subtypes of most invasive adenocarcinomas.<sup>20</sup> The subtypes included lepidic-growth predominant, acinar predominant, papillary predominant, micropapillary predominant, and solid predominant types. Each predominant type can lead to a different spectrum of prognosis. Some studies reported that lepidic-predominant adenocarcinomas are low grade; acinar and papillary tumors are intermediate grade; solid and micropapillary tumors are high grade.<sup>21</sup> We presumed that the wide range of histologic grades of adenocarcinoma of the lung caused a wide range of consequences in lung cancer survival. Although adenocarcinomas are expected to show poor survival than other cell types of NSCLC, the HR of adenocarcinoma was not significantly different from the wide-range CI.

There were a few limitations in this study. First, our study retrospectively enrolled patients based on the electronic chart review, and some extent of selection bias or confounding factors could be involved in this process. When we see a prospective lung cancer

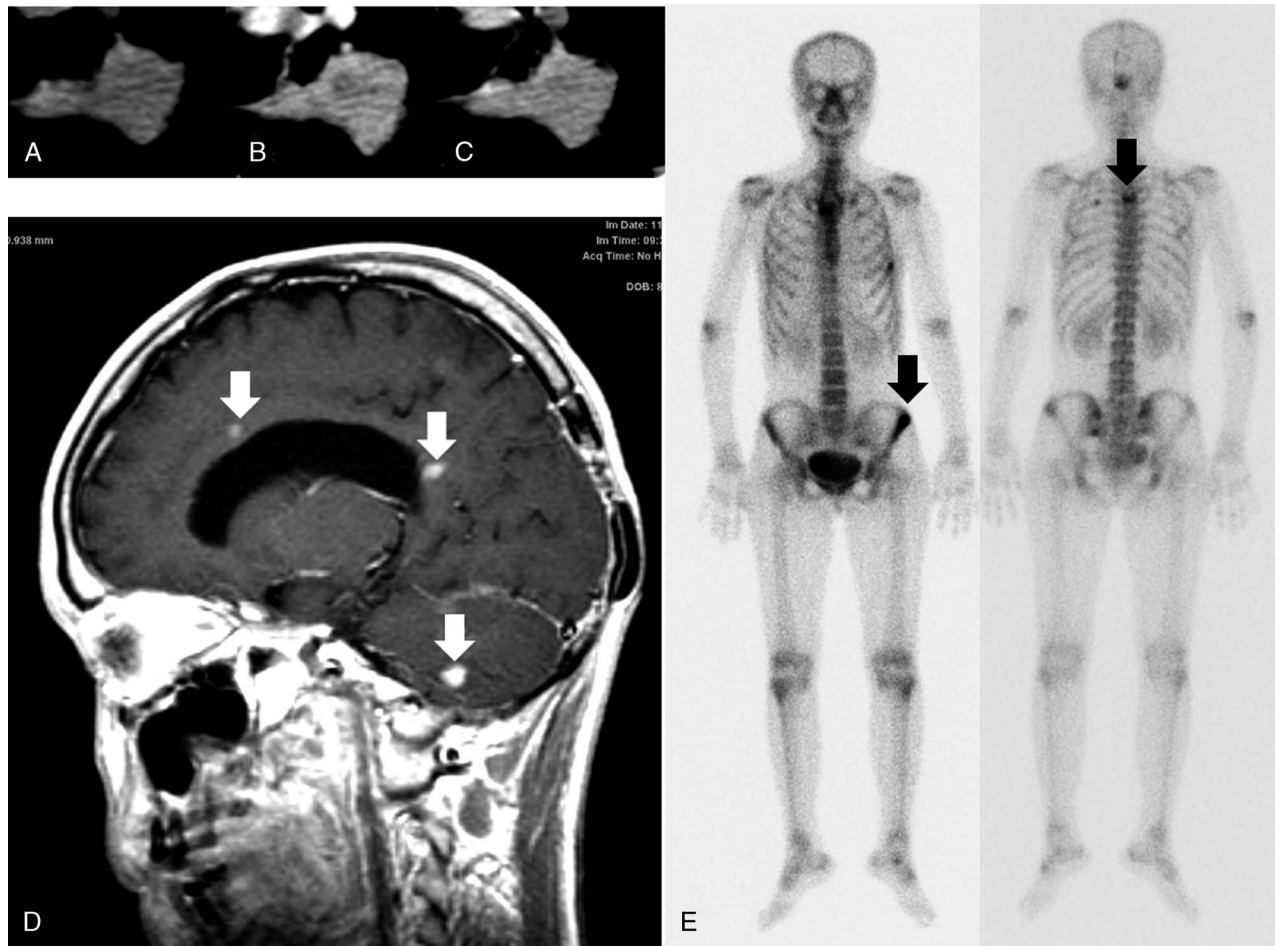


**FIGURE 4.** A 34-year-old woman with T1b N0 M0 adenocarcinoma. The attenuations of tumor nodule on dynamic contrast-enhanced CT were 23.3 HU on precontrast image (A), 105.7 HU on 30 seconds (B), and 65.4 HU on 15 minutes (C) after contrast administration. Peak enhancement was 105.7 HU, and NE was 82.4 HU. After 6 months of the curative surgery metastasis of the brain (D; white arrows on brain MR) and bone (E; black arrows on bone scan) developed. The patient died after 24 months of the curative surgery.

screening study like the international early lung cancer action project, they did CT screening for lung cancers in 31,567 patients. Three hundred two patients underwent surgical resection and confirmed to have stage I lung cancers.<sup>22</sup> One hundred thirty-nine patients underwent surgery for lung cancer and were confirmed to have stage IA lung cancers in our study. The number of 139 patients who were enrolled in our study was about half compared with this large-scale prospective screening study, whereas the process—from clinically suspected malignant solitary pulmonary nodule to surgery—was not different from this prospective study.

Second, the measured value of HU on CT was used as an indirect marker of neoangiogenesis but is not the same as the direct measurement of MVD of surgical specimens. On the other hand, these quantitative imaging markers from dynamic helical CT or perfusion magnetic resonance imaging have advantages over direct markers from pathology. Imaging markers can be measured noninvasively, repeatedly, and quantitatively. Therefore, they can be used as prognostic indicators at the initial staging workup but also used as quantitative markers when response evaluations are needed.

We proved PE on dynamic CT was an independent prognostic indicator for the death of patients with stage IA NSCLC. The PE of 90 HU or higher predicts a higher risk of survival after curative surgery for stage IA NSCLC. This result may suggest that more intensive treatment consideration such as antiangiogenic

agents or closer follow-up monitoring for progression might be needed in patients with aggressive tumor angiogenesis, even if they underwent curative surgery for early-stage lung cancers. A further prospective randomized clinical trial is needed to support this treatment strategy for early-lung cancers.

## REFERENCES

1. Bergers G, Benjamin LE. Tumorigenesis and the angiogenic switch. *Nat Rev Cancer.* 2003;3:401–410.
2. Zhao C, Yang H, Shi H, et al. Distinct contributions of angiogenesis and vascular co-option during the initiation of primary microtumors and micrometastases. *Carcinogenesis.* 2011;32:1143–1150.
3. Fontanini G, Bigini D, Vignati S, et al. Microvessel count predicts metastatic disease and survival in non–small cell lung cancer. *J Pathol.* 1995;177:57–63.
4. Meert AP, Paesmans M, Martin B, et al. The role of microvessel density on the survival of patients with lung cancer: a systematic review of the literature with meta-analysis. *Br J Cancer.* 2002;87:694–701.
5. Des Guetz G, Uzzan B, Nicolas P, et al. Microvessel density and VEGF expression are prognostic factors in colorectal cancer. Meta-analysis of the literature. *Br J Cancer.* 2006;94:1823–1832.

6. Uzzan B, Nicolas P, Cucherat M, et al. Microvessel density as a prognostic factor in women with breast cancer: a systematic review of the literature and meta-analysis. *Cancer Res*. 2004;64:2941–2955.
7. Yi CA, Lee KS, Kim EA, et al. Solitary pulmonary nodules: dynamic enhanced multi-detector row CT study and comparison with vascular endothelial growth factor and microvessel density. *Radiology*. 2004;233:191–199.
8. Lee KS, Yi CA, Jeong SY, et al. Solid or partly solid solitary pulmonary nodules: their characterization using contrast wash-in and morphologic features at helical CT. *Chest*. 2007;131:1516–1525.
9. Bremnes RM, Camps C, Sirera R. Angiogenesis in non–small cell lung cancer: the prognostic impact of neoangiogenesis and the cytokines VEGF and bFGF in tumours and blood. *Lung Cancer*. 2006;51:143–158.
10. Jeong YJ, Lee KS, Jeong SY, et al. Solitary pulmonary nodule: characterization with combined wash-in and washout features at dynamic multi-detector row CT. *Radiology*. 2005;237:675–683.
11. Efron B. The efficiency of Cox's likelihood function for censored data. *J Am Stat Assoc*. 1977;72:557–565.
12. Contal C, O'Quigley J. An application of changepoint methods in studying the effect of age on survival in breast cancer. *Comput Stat Data Anal*. 1999;30:253–270. ScienceDirect.
13. Wozniak AJ, Kosty MP, Jahanzeb M, et al. Clinical outcomes in elderly patients with advanced non–small cell lung cancer: results from ARIES, a bevacizumab observational cohort study. *Clin Oncol (R Coll Radiol)*. 2015;27:187–196.
14. Lynch TJ Jr, Spigel DR, Brahmer J, et al. Safety and effectiveness of bevacizumab-containing treatment for non–small-cell lung cancer: final results of the ARIES observational cohort study. *J Thorac Oncol*. 2014;9:1332–1339.
15. Sandler A, Gray R, Perry MC, et al. Paclitaxel-carboplatin alone or with bevacizumab for non–small-cell lung cancer. *N Engl J Med*. 2006;355:2542–2550.
16. Lou F, Huang J, Sima CS, et al. Patterns of recurrence and second primary lung cancer in early-stage lung cancer survivors followed with routine computed tomography surveillance. *J Thorac Cardiovasc Surg*. 2013;145:75–81; discussion 81–72.
17. Wang J, Wu N, Cham MD, et al. Tumor response in patients with advanced non–small cell lung cancer: perfusion CT evaluation of chemotherapy and radiation therapy. *AJR Am J Roentgenol*. 2009;193:1090–1096.
18. Lind JS, Meijerink MR, Dingemans AM, et al. Dynamic contrast-enhanced CT in patients treated with sorafenib and erlotinib for non–small cell lung cancer: a new method of monitoring treatment? *Eur Radiol*. 2010;20:2890–2898.
19. Tateishi U, Kusumoto M, Nishihara H, et al. Contrast-enhanced dynamic computed tomography for the evaluation of tumor angiogenesis in patients with lung carcinoma. *Cancer*. 2002;95:835–842.
20. Beasley MB, Brambilla E, Travis WD. The 2004 World Health Organization classification of lung tumors. *Semin Roentgenol*. 2005;40:90–97.
21. Travis WD, Brambilla E, Nicholson AG, et al. The 2015 World Health Organization classification of lung tumors: impact of genetic, clinical and radiologic advances since the 2004 classification. *J Thorac Oncol*. 2015;10:1243–1260.
22. International Early Lung Cancer Action Program InvestigatorsHenschke CI, Yankelevitz DF, Libby DM, et al. Survival of patients with stage I lung cancer detected on CT screening. *N Engl J Med*. 2006;355:1763–1771.